



Regular article

Evaluation of coating thickness by thermal wave imaging: A comparative study of pulsed and lock-in infrared thermography – Part II: Experimental investigation

Ranjit Shrestha, Wontae Kim*

Department of Mechanical & Automotive Engineering, Kongju National University, 1223-24 Cheonan-daero, Seobuk-gu, Cheonan-si, Chungcheongnam-do 31080, South Korea

ARTICLE INFO

Keywords:

Thermal barrier coatings
Topcoat thickness measurement
Thermal wave imaging
Pulsed thermography
Lock-in thermography
Fourier transform
Phase angle

ABSTRACT

In this work, we focused on the experimental arrangement of thermal wave imaging (TWI) methods for the quantitative evaluation of non-uniform topcoat thickness of thermal barrier coatings (TBCs). Two TWI techniques, pulsed thermography (PT) and lock-in thermography (LIT) were implemented on plasma sprayed TBCs with varied topcoat ranging from 0.1 mm to 0.6 mm. In PT, a short and high energy light pulse was applied on a sample surface whereas, in LIT, the sample surface was excited by a sinusoidal heat flux at several modulation frequencies ranging from 2 Hz down to 0.01 Hz. Furthermore, an infrared camera was used to capture the surface temperature of a thermal wave that propagated into the sample and the effect of the applied heat flux in both techniques was analyzed by Fourier transform. The results of PT and LIT techniques were compared based on the evaluated accuracy of each technique. Finally, it was concluded that both the techniques could be applied to the fast and accurate evaluation of TBCs thickness.

1. Introduction

Thermal barrier coatings (TBCs) are complex, multifunctional thick films of a refractory-oxide ceramic applied to the metallic surfaces of hot section components to protect from wear, erosion and high-temperature degradation, and to provide thermal insulation [1–3]. TBCs are now being used to provide thermal insulation to metallic components from the hot gas stream in gas-turbine engines used for aircraft propulsion, power generation, and marine propulsion [4–6]. The state-of-the-art TBCs consist of a yttria stabilized zirconia (YSZ) top coat, a thin thermally grown oxide (TGO) reaction layer and a metallic bond coat of MCrAlY on a superalloy substrate. The thermal insulation is provided by the topcoat YSZ layer deposited by either electron beam physical vapor deposition (EB-PVD) or plasma-spraying (PS) techniques [7–10]. Hence, the topcoat thickness is an essential parameter which determines the thermal insulation characteristics, stress, bonding strength, lifetime of components, costs, etc., and is important for performance evaluation [11–13]. Therefore, there is a need for non-destructive testing (NDT) techniques to monitor and control the thickness of coating.

Over the years, a variety of NDT techniques such as eddy current [14–17], ultrasonic [18–21], x-ray fluorescence [22–25], and terahertz

[26–28] has been developed for the evaluation of coatings. The choice among these techniques depends on the type of coatings, coating thickness, the substrate, the cost of instrumentation and the accuracy required [29,30]. However, these all have certain limitations such as; eddy current suffers from manual scanning; ultrasonic suffers from size and shape of the target object; x-ray is difficult to competent due to porous nature of TBCs and terahertz suffers from the requirement of a refractive index [31–34]. In this context, thermal wave imaging (TWI) often known as infrared thermography (IR) becomes a research hotspot in recent years as it has unique advantages of large detection area, fast speed, non-contact, safe and convenient operation, more coating materials and high efficiency over other inspection methods [6,35–37]. Pulsed thermography (PT) [38–42] and lock-in thermography (LIT) [43–47] are proved to be very appropriate NDT techniques for the evaluation of TBCs [48–52].

In our previous work, hereafter Part I [53], results of a systematic investigation of non-uniform TBCs using finite element model (FEM) analysis were reported. In part I, a transient FEM model was developed in ANSYS heat transfer module and stimulated by a flow of heat to simulate PT and LIT experimental procedures. The sample considered for the analysis was characterized by a steady substrate and the bond coat with varied topcoat ranging from 0.1 mm to 0.6 mm. The response

* Corresponding author.

E-mail address: kwt@kongju.ac.kr (W. Kim).

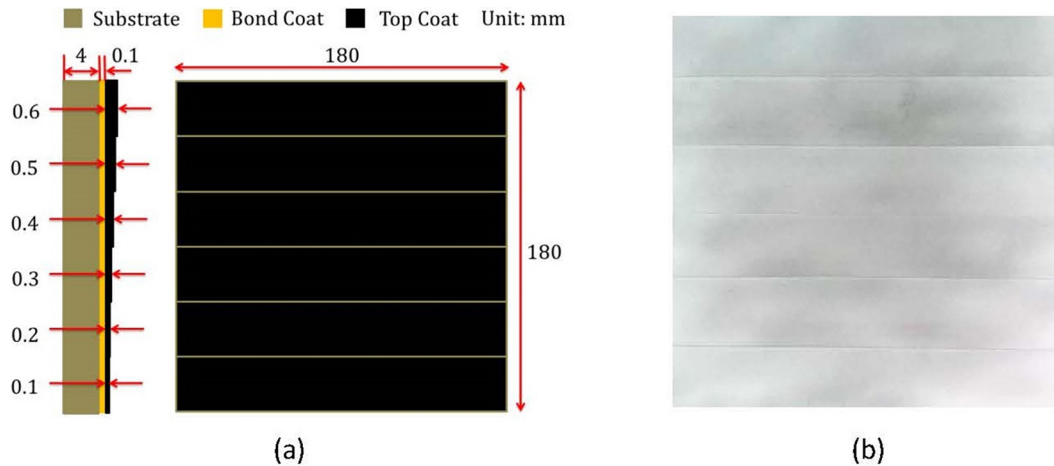


Fig. 1. TBCs test sample description, (a) Schematic illustration of the sample along with the geometry and (b) Front side of the sample.

of the thermally excited surface was recorded and analyzed by Fourier transform (FT) [54–56]. As results, we found that FEM enabled a better understanding of PT and LIT and demonstrated potential in the evaluation of TBCs thickness. In order to extend our previous study and to validate the FEM analysis results, we focused on the experimental arrangement of PT and LIT techniques. In this work, we present the experimental results and discuss them together with the results from Part I.

2. Materials and methods

2.1. Sample

Fig. 1 shows the schematic illustration of TBCs test sample along with the geometry and the front side of the sample. Nickel-based superalloy ($180 \times 180 \times 4$, in mm) plate was used a substrate. MCrAlY alloys ($M = \text{Co}, \text{Ni}, \text{or Co/Ni}$) powder by air plasma spraying (APS) process was sprayed onto the top surface of the substrate to form a bond coat of 0.1 mm. Then topcoat of Ytria-stabilized zirconia (YSZ) by APS process was applied to the bond coat surface. The thickness of topcoat was maintained in the range of 0.1–0.6 mm as shown in Fig. 1. The emissivity of YSZ-TBCs was measured and is about 0.73 [57]. The details of nanomaterials used for the preparation of TBCs can be found in the literature [58–61].

2.2. Pulse thermography (PT) experimental system

The PT system consisted of the power system, flash lamp, an infrared (IR) camera and a system controller. A power supply (BALCAR Light System, Nexus A 6400, France) utilized a flash lamp (Universal BALCAR, France) of power 6400 W-s as a heat source to launch a pulse of heat into the specimen surface. An IR camera (SC645, FLIR Systems, Sweden) with a 640×480 – pixel resolution and a wavelength of 7.5–13 μm was used to record the thermal response of the sample. An IR lens with focal length 41.3 mm was used together with the camera, which was positioned in such a way that it would fully capture the entire sample. The FLIR R&D software was used to acquire the thermal images. The camera frame rate was set to 50 frames per second.

2.3. Lock-in thermography (LIT) experimental system

The LIT system consisted of a lock-in module, a heat source, an IR camera, and a system controller [62–64]. A programmable function generator (Agilent 33210A, Malaysia) was used for the generation of sine waves. Two halogen lamps (OSRAM, Medium Flood, China) of 1 kW each were used as a heat source. The LIT system (Answer Tech,

Republic of Korea) was used to synchronize the input and output signals. The same infrared camera as specified in PT experimental system was used for LIT experimental investigation.

3. Results and discussions

3.1. PT results

The PT experimental investigation was conducted in reflection mode. The pulse heating time was set as 10 ms followed by cooling time of 5 s. Fig. 2 shows the surface temperature responses of TBCs with respect to variation in thickness of topcoat. During the measurement of temperature, a region of interest (ROI) was selected, and the temperature of each pixel within the ROI was averaged to reduce the noise and the errors in the measurement. Fig. 3 shows the pulsed thermal images acquired at a different time interval. As can be seen in Figs. 2 and 3, the temperature rise was faster than its decay because of very short impulse time. As the time passes, due to thermal diffusion in all directions, the temperature on the sample surface tended to reach equilibrium. It was also observed that the surface temperature was relatively high at large thickness.

The whole thermal data were processed by FT to compute phase angle. Fig. 4 shows the computed phase image and Fig. 5 shows the plot of phase angle with respect to variation in topcoat thickness. As can be seen in Figs. 4 and 5, phase angle decreased with the increasing coating thickness. However, notably in Part I, the phase angle increased with

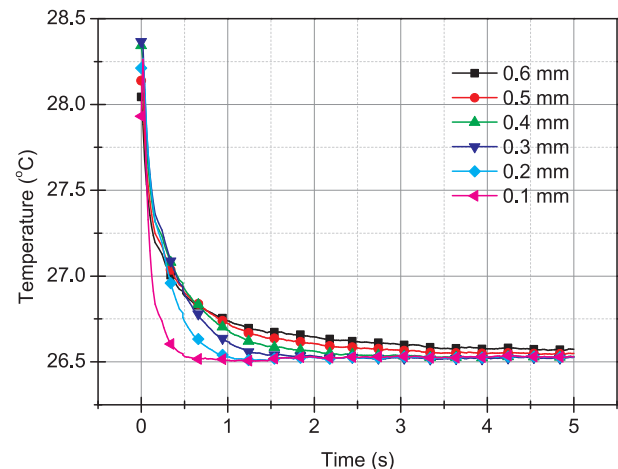


Fig. 2. PT Experimental surface temperature evolution curves of TBCs with respect to variation in the thickness of topcoat.

Download English Version:

<https://daneshyari.com/en/article/8145541>

Download Persian Version:

<https://daneshyari.com/article/8145541>

[Daneshyari.com](https://daneshyari.com)